1975

# Design and Calibration of a Three Component, Single Element, Wind Tunnel Force Balance

Victor W. Tisdel
*University of Central Florida*

# DESIGN AND CALIBRATION OF A THREE COMPONENT, SINGLE ELEMENT, WIND TUNNEL FORCE BALANCE

BY

VICTOR W. TISDEL
B.S., Embry-Riddle Aeronautical University, 1967

RESEARCH REPORT

Submitted in partial fulfillment of the requirements
for the degree of Master of Science in Engineering
in the Graduate Studies Program of
Florida Technological University

Orlando, Florida
1975

ACKNOWLEDGMENTS

I would like to gratefully acknowledge my indebtedness to Professors R. C. Rapson, C. E. Nuckolls, and J. K. Beck of Florida Technological University for their valuable suggestions and criticisms, without which this report would not have been possible.

Victor W. Tisdel

# FORWARD

The topic of this paper is the design and analysis of a three component, single element, wind tunnel force balance. This force balance was designed and built by Victor W. Tisdel, for Embry-Riddle Aeronautical University at Daytona Beach, Florida for use in their low speed, three foot by four foot wind tunnel.

## ABSTRACT

The purpose of this paper was to design a simplified wind tunnel force balance for use in elementary aerodynamics/wind tunnel laboratory courses. The applied loads and moments were determined to be as follows:

- The design lift force is ± 20 pounds
- The design drag force is ± 10 pounds
- The design pitching moment is ± 20 inch-pounds.

The force balance output accuracy was arbitrarily set at ± 5% since this would be sufficient for preliminary student work.

The results of this work are as follows:

- The force balance is fabricated from a single bar of 2024 aluminum, machined and bent into an "L" shape.
- The applied forces and moments are sensed by strain gages bonded to machined surfaces on the bar.
- The output of the strain indicator equipment is transformed into uncorrected forces and moments by

a system of three equations.

- The uncorrected forces and moments are transformed into true forces and moments by a system of force balance interaction equations.

- The design values for lift, drag, and pitching moment remain the same as originally proposed.

- The output error in lift is determined to be ± 3.5%.

- The output error in drag and pitching moment are determined to be ± 10%.

The prototype has been in use for several months and its operation has been completely satisfactory.

CONTENTS

## LIST OF ILLUSTRATIONS

## LIST OF SYMBOLS

| | |
|---|---|
| $S$ | Fiber Stress |
| $I$ | Moment of Inertia |
| $L$ | Lift |
| $D$ | Drag |
| $M$ | Moment, Pitching moment |
| $\Delta R$ | Strain Indication |
| $S_1$, $S_2$, $S_3$ and $S_4$ | Beam Dimensions |
| $C_1$ through $C_6$ | Beam Constants |
| $C_7$ through $C_{13}$ | Calibration Constants |
| $C_{14}$ through $C_{23}$ | Interaction Constants |
| $M_1$, $M_2$ and $M_3$ | Flexure Moments |
| $M_y$ | Yielding Moment |
| $M_f$ | Full Plastic Moment |
| $M_r$ | Residual Moment |

# CHAPTER I

## INTRODUCTION

The subject of this paper is the design and fabrication of a single element, three degree of freedom, wind tunnel force balance. The need for such a force balance originated from the operational requirements of the Embry-Riddle Aeronautical University 3 ft. by 4 ft. wind tunnel. This wind tunnel is used to support academic courses in aerodynamics, in much the same way that physical science and chemistry laboratories support their lecture classes. With this in mind, extreme accuracy and six degrees of freedom were exchanged for mobility and versatility.

There are, of course, many force balances available, all of them excellent in operation and very expensive. They fall into two general types; the platform type which is permanently installed under the wind tunnel test section and the internal type which is generally designed for a specific model. This design utilizes the internal type of construction while having it operate as an external element, to increase its versatility.

The choice of a single element is to reduce the material and man hours required for fabrication of the balance and to decrease its susceptibility to damage while

being handled. While there are no tolerances set for its fabrication, care should be used during its manufacture to increase the calibration sensitivity.

This report does not include any items such as model design, model to balance interface, etc., for these are separate topics worthy of discussion in their own right. The same is true for force balance support items such as pitch changing mechanisms, strain indicators and switching and balancing units.

Finally, one must realize that the accuracy of any apparatus is only as good as the calibration procedure. The calibration procedure presented in this report is a general one, used for the general development of the design.

## CHAPTER II

## DESIGN OBJECTIVES

Most external wind tunnel force balances are designed to measure the maximum loads impressed upon the largest model a test section can accomodate at its maximum dynamic pressure. Internal wind tunnel force balances are designed to accomodate a given model at a given maximum dynamic pressure. Although this force balance resembles an internal type, it is designed according to external balance design criteria.

The wind tunnel at Embry-Riddle has a 11.8 $ft^2$ test section and a turbulence factor of 1.3 at a test section velocity of 100 ft. per second. Since the balance is going to be used by undergraduate students for their own designs and manufactured models, their model wing span is restricted to a maximum of 24 inches to minimize wall effects and reduce the cost of the model. Assuming a maximum lift coefficient of 2.4 and a minimum aspect ratio of 6, the maximum lift force would be 19.3 lbs. The balance would be used for other purposes as well, so the minimum drag-to-lift ratio is arbitrarily set at 1:2 and likewise the maximum pitching moment, in inch-pounds, is set equal to the lift.

The resulting balance design loads are:

$$\text{Lift} = \pm 20 \text{ pounds}$$
$$\text{Drag} = \pm 10 \text{ pounds} \qquad (2:1)$$
$$\text{Moment} = \pm 20 \text{ inch-pounds}$$

At Embry-Riddle, there are often as many as three courses requiring the use of the wind tunnel during each week. This means that the wind tunnel operator must be able to remove and install experiments frequently. It also means that the calibration of the balance would best be accomplished outside the test section. For these reasons the force balance was designed to be permanently mounted to a base plate so that the balance with its base plate could be moved from the calibration bench to the test floor without disturbing the calibration. The dimensions of the test section dictates that the maximum height of the balance be 24 inches and the length of the balance be 18 inches. It was assumed that the frequency of the vibration of the test section floor would be high enough that the damping of the meter movement of the strain indicator would render it unmeasurable.

The fabrication of the force balance beam must be kept simple. It was decided that the beam would be one piece, formed in a right angle and requiring only one type of machining operation. Only one type of strain gage is used and they are unobstructed for easy installation. To further simplify the strain gage installation and

alignment, only two gages are used per flexure, one on each flat, and a half bridge setup is used with the stain indicator, see Figure 2-1. The only machines required are a vertical mill and a drill press, however, the flexure flats can be put in by hand with a file. There is no implied tolerance for the flats except that the flats of a particular flexure should be as parallel as possible. This means that the moments measured at the flexures can not be compared directly.

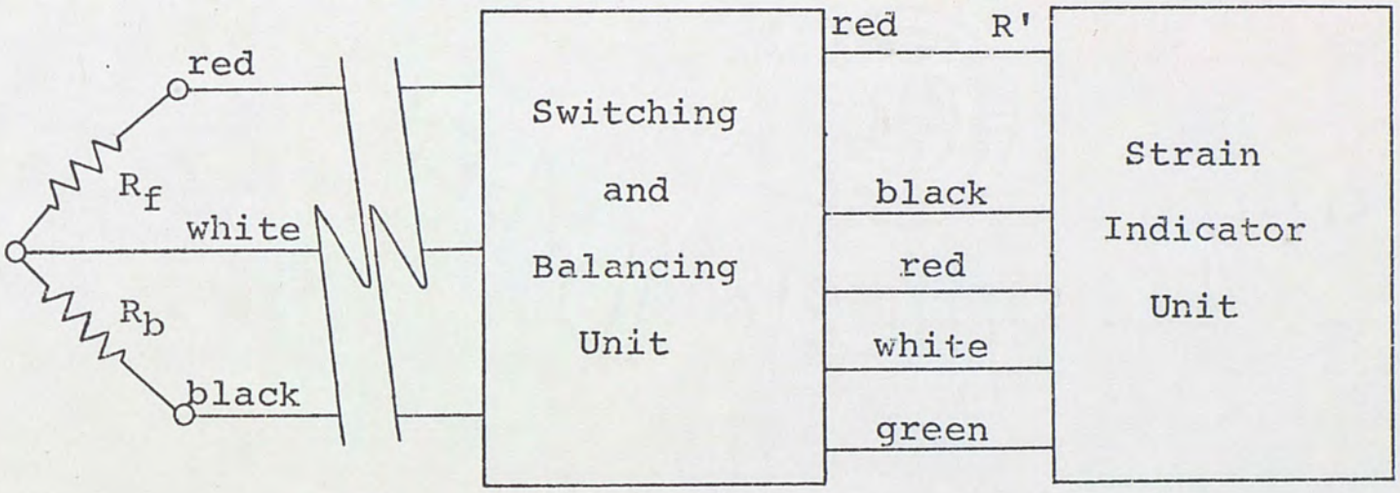


Figure 2-1, Flexure to Strain Indicator Wiring.

To simplify data reduction and balance calibration, a system of equations is used that will convert strain indicator readings directly into output loads and moments. While it is desirable to employ these equations in a computer program, they can, and are often used in hand calculations.

The accuracy of the system depends on many factors.

The net result is that the greater the accuracy the larger the cost. To keep the costs down, the accuracy is arbitrarily set at ± 5% of the applied loads and error curves are developed.

# CHAPTER III

## DESIGN ANALYSIS

The design is based on a cantilever beam bent into an "L" shape. It is structurally supported at the base, which is a plate fastened to the test section floor, and the model is attached at the top. The base has one flexure and the vertical part has two flexures, one near the bottom and the other near the top. Figure 3-1 shows the basic configuration. The principle is that all forces and moments to be measured will appear as various combinations of moments at the flexures. These moments are measured by strain indicating equipment and the desired loads and moments are separated by suitable mathematic relations. Any model attachment and control apparatus is omitted in this report because it is not relevant to the balance design.

The requirement that the balance be easily fabricated would be satisfied if the machining of the flexures is not critical. This is accomplished by not requiring that the output of the strain gage pairs at the flexures be compared with one another directly. In fact, since

$$S = \frac{(M)(y)}{I} \qquad (3\text{-}1)$$

we only need to use

$$M = KS = K_1 \text{ (S.G. Indication)} \qquad (3\text{-}2)$$

and $K_1$ is determined during calibration. This is especially desirable since it means that different values of $K_1$ can be used for each flexure. It also means that $K_1$ need not be a constant but, in fact, may be a function of the loads and/or the deflections affecting the flexure. The machining of the flexures is therefore not critical and is controlled primarily by the required strength of the flexure.

The sizing of the balance beam and selection of material is the next logical step of development. In general, there are two materials used in balance construction, aluminum and steel. Steel is by far the most widely used, however because of the light loads that were expected and because of its workability, aluminum was chosen. Also, the mass-inertia characteristics and high thermal conductivity of aluminum helps reduce beam vibrations and strain gage thermal drift. Fiber stresses in aluminum beams should not exceed 10,000 psi (5).

Considering the diagram in Figure 3-1, the moments are proportional to the strain indications, $\Delta R$, and can be written

$$\begin{aligned} M_1 &\sim \Delta R_1 \\ M_2 &\sim \Delta R_2 \\ M_3 &\sim \Delta R_3 \end{aligned} \qquad (3\text{-}3)$$

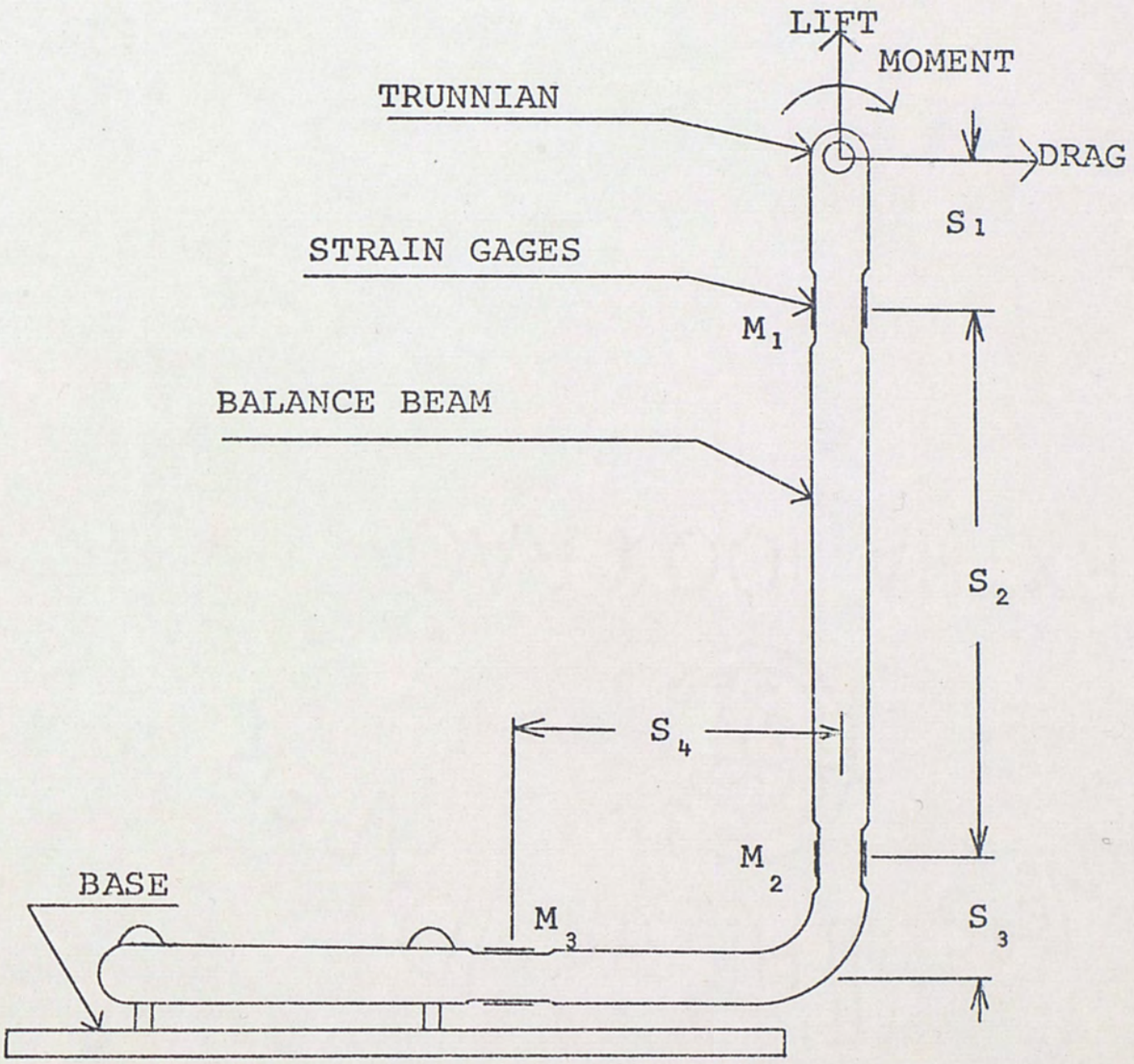


Figure 3-1, Force Balance Configuration.

also, the force balance equations are written

$$M_1 = M + S_1 D$$

$$M_2 = M + (S_1 + S_2) D \tag{3-4}$$

$$M_3 = M + (S_1 + S_2 + S_3) D - S_4 L$$

from which

the resulting force equations are obtained

$$D = C_1 (M_1 - M_2)$$

$$M = C_2 M_1 - C_3 M_2 \tag{3-5}$$

$$L = C_4 M_1 - C_5 M_2 - C_6 M_3$$

where

$$C_1 = \frac{1}{S_2} \tag{3-6}$$

$$C_2 = 1 - \frac{S_1}{S_2} \tag{3-7}$$

$$C_3 = - \frac{S_1}{S_2} \tag{3-8}$$

$$C_4 = \frac{2S_2 + S_3}{S_2 S_4} \tag{3-9}$$

$$C_5 = \frac{S_2 + S_3}{S_2 S_4} \tag{3-10}$$

$$C_6 = \frac{1}{S_4}. \tag{3-11}$$

The actual value of the S's is important only to the initial sizing of the balance beam because the values of the C's are determined during the balance calibration.

The moment $M_3$ will produce the largest fiber stress and it is determined from the expected loads by

$$M_3 = M + (S_1 + S_2 + S_3) D - S_4 L. \tag{3-12}$$

The fiber stress is determined by

$$S = \frac{M_3 y}{I} \qquad (3\text{-}13)$$

and the length between flexures and the beam cross section is adjusted to maintain the 10,000 psi stress.

For the balance and strain indicator system, the following equations are obtained:

$$D' = C_1(K_1\Delta R_1 - K_2\Delta R_2)$$

$$M' = C_2K_1\Delta R_1 - C_3K_2\Delta R_2 \qquad (3\text{-}14)$$

$$L' = C_4K_1\Delta R_1 - C_5K_2\Delta R_2 - C_6K_3\Delta R_3.$$

The constant products are combined into single products, resulting in:

$$D' = C_7\Delta R_1 - C_8\Delta R_2 \qquad (3\text{-}15)$$

$$M' = C_9\Delta R_1 - C_{10}\Delta R_2 \qquad (3\text{-}16)$$

$$L' = C_{11}\Delta R_1 - C_{12}\Delta R_2 - C_{13}\Delta R_3 \qquad (3\text{-}17)$$

where $C_7$ through $C_{13}$ are determined in calibration by separate load application. The notations $L'$, $D'$, and $M'$ are now used to indicate raw data that has not been corrected for load interaction.

Since the stress-strain curve of aluminum is essentially linear in its elastic range, the indicated load will include the true load plus linear components of the other applied loads. This results in the following system of equations:

$$L' = L + \frac{\partial L}{\partial D}D + \frac{\partial L}{\partial M}M$$

$$D' = \frac{\partial D}{\partial L}L + D + \frac{\partial D}{\partial M}M \qquad (3\text{-}18)$$

$$M' = \frac{\partial M}{\partial L}L + \frac{\partial M}{\partial D}D + M$$

which may be written

$$\begin{Bmatrix} L' \\ D' \\ M' \end{Bmatrix} = \begin{pmatrix} \frac{\partial L}{\partial L} & \frac{\partial L}{\partial D} & \frac{\partial L}{\partial M} \\ \frac{\partial D}{\partial L} & \frac{\partial D}{\partial D} & \frac{\partial D}{\partial M} \\ \frac{\partial M}{\partial L} & \frac{\partial M}{\partial D} & \frac{\partial M}{\partial M} \end{pmatrix} \begin{Bmatrix} L \\ D \\ M \end{Bmatrix} \qquad (3\text{-}19)$$

Inverting the matrix gives the desired solution:

$$\begin{Bmatrix} L \\ D \\ M \end{Bmatrix} = (B)^{-1} \begin{Bmatrix} L' \\ D' \\ M' \end{Bmatrix} \qquad (3\text{-}20)$$

where

$$(B) = \begin{pmatrix} \frac{\partial L}{\partial L} & \frac{\partial L}{\partial D} & \frac{\partial L}{\partial M} \\ \frac{\partial D}{\partial L} & \frac{\partial D}{\partial D} & \frac{\partial D}{\partial M} \\ \frac{\partial M}{\partial L} & \frac{\partial M}{\partial D} & \frac{\partial M}{\partial M} \end{pmatrix} \qquad (3\text{-}21)$$

The gradients $\frac{\partial L}{\partial D}$, $\frac{\partial L}{\partial M}$, etc.; are obtained during calibration by the application of load pairs. The result is the following system of equations:

$$L = C_{14}\, L' + C_{16}\, D' + C_{17}\, M' \qquad (3\text{-}22)$$

$$D = C_{18}\, L' + C_{19}\, D' + C_{20}\, M' \qquad (3\text{-}23)$$

$$M = C_{21}\, L' + C_{22}\, D' + C_{23}\, M' \quad . \qquad (3\text{-}24)$$

The constants $C_{14}$ through $C_{23}$ are independent of the balance application.

The balance equations to perform the required task have now been obtained. With an unknown applied lift, drag and pitching moment, $\Delta R_1$, $\Delta R_2$ and $\Delta R_3$ are obtained from the strain indicator. These $\Delta R$'s are substituted into

$$D' = C_7 \Delta R_1 - C_8 \Delta R_2$$

$$M' = C_9 \Delta R_1 - C_{10} \Delta R_2$$

$$L' = C_{11} \Delta R_1 - C_{12} \Delta R_2 - C_{13} \Delta R_3 \quad .$$

The raw loads are then substituted into

$$L = C_{14} L' + C_{16} D' + C_{17} M'$$

$$D = C_{18} L' + C_{19} D' + C_{20} M'$$

$$M = C_{21} L' + C_{22} D' + C_{23} M'$$

and the values of the applied load are obtained.

## CHAPTER IV

## FORCE BALANCE FABRICATION

The force balance design guidelines are the following:

- The maximum length and height of the apparatus as installed in the wind tunnel test section
- The expected maximum loads applied to the balance
- The desire to use commercially available material
- The fabrication capability of the builder.

With these conditions in mind it was decided that the balance beam would be fabricated of 2024 aluminum bar stock of round cross section. At least one-half of the base length is dedicated to the attachment of the base plate. This means the moment at the base plate attachment created by simultaneous application of the maximum loads on the balance trunnian is 440 in-lb. This is assuming the balance trunnian is at the test section centerline and the worst loading condition, i.e. positive

drag and moment and negative lift.

The round cross section has flats milled into it to create the flexures. The cross section is shown in Figure 4-1 and the derivation of its moment of inertia is as follows:

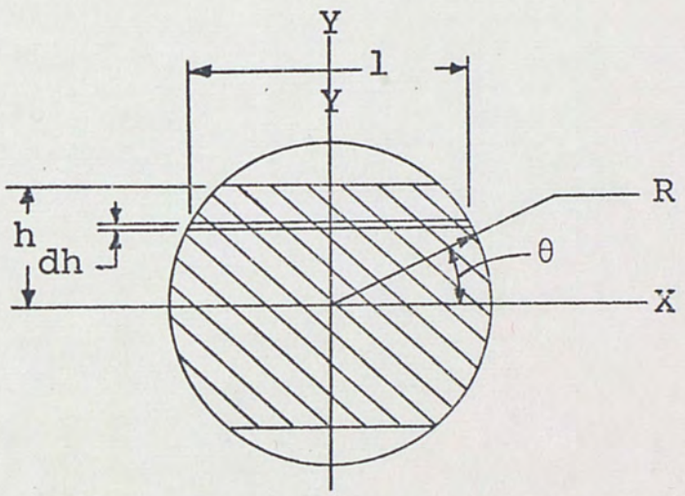


Figure 4-1, Flexure Cross Section.

$$I_x = \int_{-h}^{h} y^2 dA = \int_{-h}^{h} y^2 l dh \qquad (4\text{-}1)$$

where:

$$y = R \sin\theta$$

$$l = 2R \cos\theta$$

$$dh = R \cos\theta \, d\theta$$

so

$$I_x = 2R^4 \int_{-\theta}^{\theta} \sin^2\theta \cos^2\theta d\theta$$

$$= -\frac{R^4}{4} \{\tfrac{1}{4}\sin 4\theta - \theta\}_{-\theta}^{\theta} \quad . \qquad (4\text{-}2)$$

Since at least a 0.3 inch wide flat is needed to attach the strain gage, the angle $\theta$ becomes

$$\theta = \frac{\pi}{4} - \arctan \frac{0.15}{R} \quad . \tag{4-3}$$

Combining equations (3-1), (4-2) and (4-3), and the recommendation that the stresses under strain gages mounted on aluminum remain below 10,000 psi results in a bar diameter of .768 inches.

Since the aluminum bar must be bent in a $90^{o}$ angle to form the structural part of the force balance beam, the strength of the bend must be investigated. The applied moment required to initiate yielding of the extreme fibers of the bar is (1)

$$M_y = \sigma_y \frac{\pi r^3}{4} = (47,000)\left(\frac{\pi}{4}\right)\left(\cdot\frac{768}{2}\right)^3 = 2090.17 \text{ in-lb.} \tag{4-4}$$

The moment required to attain full plastic bending of the bar is (4) 170% of the yielding moment, or

$$M_f = 1.7\ M_y = 3553.29 \text{ in-lb.} \tag{4-5}$$

Releasing the bar is equivalent to applying a negative moment equal in magnitude to the moment required for full plastic bending. It is assumed that this negative moment produces only elastic strains (4) and therefore a residual negative moment of

$$M_r = M_f - M_y = 1463.12 \text{ in-lb.} \tag{4-6}$$

is induced in the bar. This means the

maximum allowable moment that can be applied in this same direction, before yielding occurs is

$$M_m = M_y - M_r = 6271.05 \text{ in-lb.} \qquad (4\text{-}7)$$

Now, the moment caused by the worst applied loading condition that occurs at the bend is 201.3 in-lb. This yields a factor of safety of

$$F.S. = \frac{627.05}{201.3} = 3.12. \qquad (4\text{-}8)$$

This is the smallest factor of safety of the beam and exceeding it would only straighten the beam out, thereby unloading it. This factor of safety is considered satisfactory.

An estimate of the deflection of the force balance beam is desirable because the slope at the model end of the beam gives the change in model angle of attack and the linear deflection of the model end of the beam gives the minimum clearance between the force balance beam and the force balance windshield. Using the method of superposition and elementary beam deflection formulae of (4) the angular change at the end of the beam is

$$\Delta\theta = 1.33^{o} \qquad (4\text{-}9)$$

and the linear deflection is

$$\delta = .129 \text{ inch.} \qquad (4\text{-}10)$$

These are computed under the worst loading conditions. These values are quite satisfactory for the use intended.

The commercially available, aluminum bar stock diameters, near the required diameter of .768 inches are .75 and .8125 inch diameters. For the prototype, the .75 inch diameter stock was selected and the force balance shown in Appendix A was fabricated. The depth of the flats is 0.05 inches giving a width of .38 inches for mounting the stain gages. The moment of inertia as determined from equation (4-2) is

$$I_x = .01252 \text{ in}^4 \tag{4-11}$$

and the maximum stress, from equation (3-1) is

$$S = \frac{(341.25)(.325)}{.01252} = 8858 \text{ psi.} \tag{4-12}$$

The selection of the .75 inch diameter bar also changed the following:

- $M_y = 1946.62$ in-lb
- $M_f = 3309.27$ in-lb
- $M_r = 1362.64$ in-lb
- $M_m = 583.98$ in-lb (4-13)
- F.S. = 2.9
- $\Delta\theta = 1.46^o$
- $\delta = .142$ inch.

Some general rules concerning the selection of strain gages are (3):

- Adequate strain must be provided under the gages for the design loads (larger than 600 micro-inches per inch)
- Gages should be matched for gage factor and resistance
- The longest gage length possible should be used.

The strains under the gages in this installation, for the maximum design loads considered, are:

- 116 microinches per inch for $M_1$
- 419 microinches per inch for $M_2$
- 840 microinches per inch for $M_3$.

This indicates that the depth of the flats of flexures 1 and 2 should be larger than the depth of the flat at flexure 3. This, however, was not done with the prototype because of the desirability of simplified machining requirements and because of the material required above flexure 1 for the trunnian attachment. However, this caused a decrease in accuracy for sensing drag and pitching moment.

The strain gages used are general purpose, constantan foil strain gages with a polyimide film backing. The gages are mounted with their longitudinal axes

parallel to the beam center line and are centered on the flats. They are wired in parallel to form one-half of the bridge of the stain indicator. The gages were bonded with a 100% solids epoxy mixture and oven cured for two hours at 150°F as suggested in the bonding instructions.

Finally the force balance is attached to its base plate and installed on the calibration bench. The caligration bench is a solid structure from which loads can be applied to the trunnian, either singly or in combination. The calibration apparatus is shown in Figure 4-2. Calibrated masses from Embry-Riddle's Physical Science Department were used to apply the calibration loads. The loads are through cables over pulleys to the trunnian and by keeping the cables long, misalignment errors are reduced.

The calibration proceeds as follows:

- Apply single component loads to the trunnian, up to the maximum expected wind tunnel loads. Plot curves of load vs strain indicator readings and determine the linear range. Within this linear range use the load/indicator readings to determine the constants $C_7$ through $C_{13}$ of equations (3-25), (3-26) and (3-27).

- The balance is then loaded in component pairs

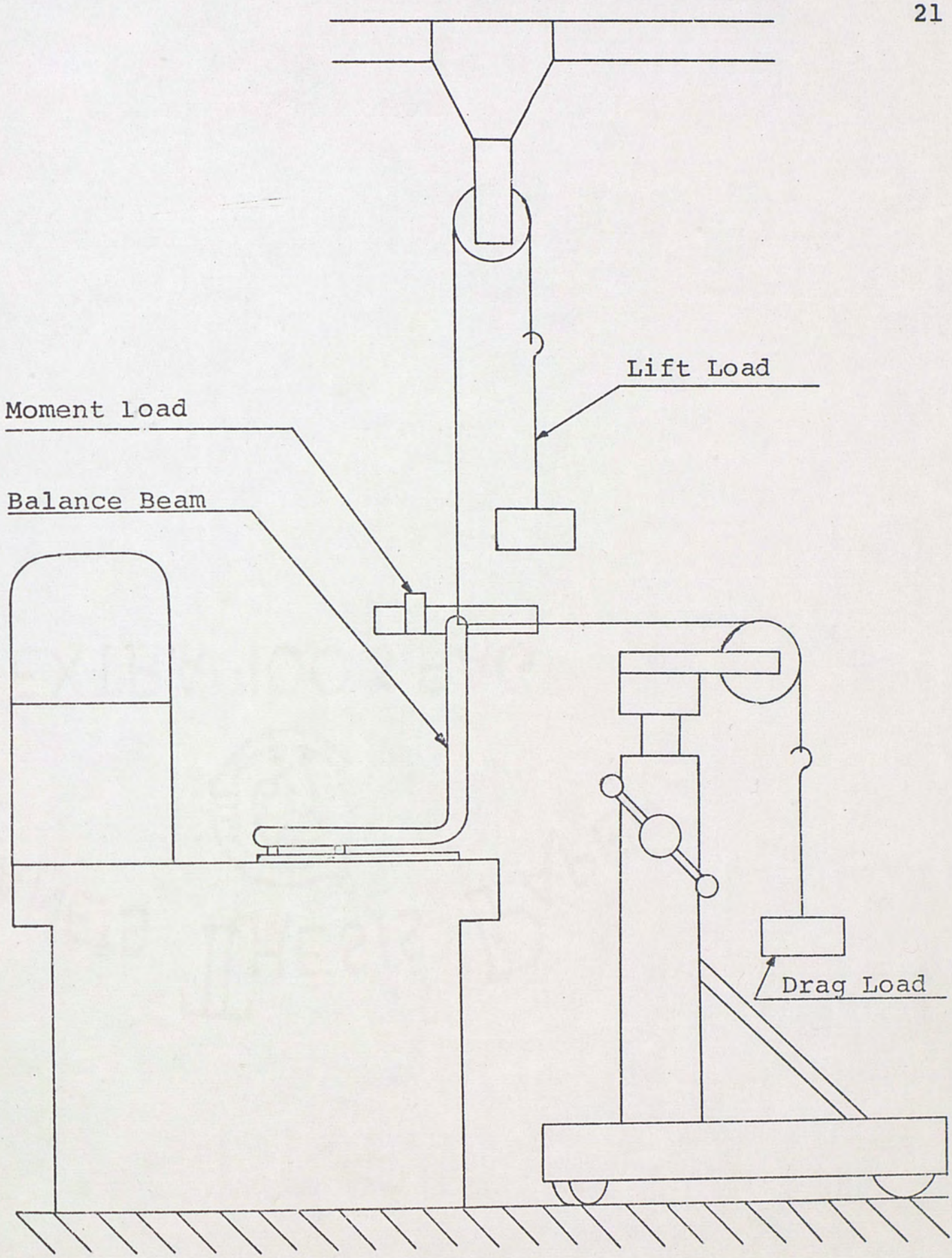


Figure 4-2, Force Balance Calibration Apparatus.

and the results of equations (3-25), (3-26) and (3-27) are combined with equations (3-18) to determine the load interaction gradients.

- The gradients are put into matrix (3-19) and inverted to form the matrix equation (3-20). The final balance equations (3-22), (3-23) and (3-24) are then formed.

- The balance is then loaded with combinations of all three components and equations (3-22), (3-23) and (3-24) are then used to create error curves.

## CHAPTER V

## EXPERIMENTAL RESULTS

In the preceding chapters the reason for the force balance, its analysis and design, its fabrication and calibration were discussed. In this chapter the balance as shown in Appendix A is calibrated. Calibration tables and graphs are given in Appendix C and the results are presented in the following paragraphs.

The graphs of balance indication versus applied loading shows all variations to be linear, except for two cases which will be discussed later. The values used for the determination of the constants $C_7$ through $C_{13}$ in equations (3-25), (3-26) and (3-27) are noted on the graphs and listed below.

| Lift | Drag | Moment | $\Delta R_1$ | $\Delta R_2$ | $\Delta R_3$ |
|---|---|---|---|---|---|
| 19.845 (9 Kg) | 0 | 0 | 10 | 21 | -692 |
| 0 | 6.615 (3 Kg) | 0 | 107 | 516 | 632 |
| 0 | 0 | -10 | -50 | -50 | -50 |

Table 5-1

The result of applying the data of Table 5-1 to equations (3-25), (3-26) and (3-27) is:

$$D' = .0162(\Delta R_2 - \Delta R_1) \qquad (5\text{-}1)$$

$$M' = .2455\Delta R_1 - .0509\Delta R_2 \qquad (5\text{-}2)$$

$$L' = -.008\Delta R_1 + .0362\Delta R_2 - .0282\Delta R_3 \qquad (5\text{-}3)$$

where

$$\Delta R = R_0 - R_i \qquad (5\text{-}4)$$

and

$R_0$ = initial balance zero

$R_i$ = final balance indication.

The equations (5-1), (5-2) and (5-3) are then used to compute the force balance output for the component pairs. The output of the force balance is then plotted versus the input of one known load for fixed values of the other known loads. These graphs are shown in Appendix C. These curves are then faired with a straight line, so as to minimize the error, and the gradients of these curves are determined and substituted into equations (3-18). The gradients used are listed below in Table 5-2.

| | | |
|---|---|---|
| $\frac{\partial L}{\partial L} = 1.009$ | $\frac{\partial L}{\partial D} = -.02$ | $\frac{\partial L}{\partial M} = .007$ |
| $\frac{\partial D}{\partial L} = .007$ | $\frac{\partial D}{\partial D} = 1.05$ | $\frac{\partial D}{\partial M} = .003$ |
| $\frac{\partial M}{\partial L} = .100$ | $\frac{\partial M}{\partial D} = .033$ | $\frac{\partial M}{\partial M} = 1.06$ |

Table 5-2

The values of Table 5-2 are then formed into matrix (B) and inverted to form equations (3-20). The final result is the balance interaction equations (3-22), (3-23) and (3-24. These equations, as determined from the test data are shown below.

$$L = .9916L' + .0191D' - .0066M' \quad (5\text{-}5)$$

$$D = -.0063L' + .9523D' - .0027M' \quad (5\text{-}6)$$

$$M = -.0933L' - .0314D' + .9441M' \quad (5\text{-}7)$$

The procedure to use the force balance is quite simple. For a given set of balance outputs, i.e. $\Delta R$'s, equation (5-1), (5-2) and (5-3) are used to compute the raw balance force and moment values. These raw balance values are substituted into equations (5-5), (5-6) and (5-7) and the final balance output is computed. A computer program written in Dartmouth Basic Language is presented in Appendix D, which will compute the final output from the input of the strain gage indicator readings (the $R_i$'s).

Because of the nonlinearity of the balance interaction curves, further correction of the final balance output may be desired. This is accomplished by drawing balance error curves from the calibration data.

# CHAPTER VI

## ERROR ANALYSIS

As noted in Chapter V, the gradient curves are troublesome because they are nonlinear. Part of the reason for the nonlinear curves is that the balance beam deflects under load. This deflection moves the application point of the lift and drag loads. This means that length $S_4$ of Figure 3-1 is changing according to the loading condition. In the derivation of the balance equations $S_4$ was considered constant and therefore causes an output error.

Another reason for nonlinear gradient curves is that lift is not considered during the computation of the constants of the drag and moment equations while both drag and moment are included in the computation of the constants in the lift equation. Consequently, the error in lift is small, about 3.5%, and the drag and moment errors vary, sometimes becoming as large as 10%.

Moment output is effected by both lift and drag because its strain indicator reading is more sensitive than the indicator readings for lift and drag. Since the measured moment computation depends upon the removal of the moment produced by drag on any given flexure and

drag errors are produced when lift is applied, the family of error curves shown in Figure E-2 were produced. These curves give the amount of moment to be added to the raw moment output as a function of raw drag output and for various values of raw lift output.

When lift is applied to the force balance, the beam is deformed as shown in Figure 6-1. This deformation produces a couple between the flexures that measure the moments $M_1$ and $M_2$. The couple is the same type as the couple used to measure drag and therefore produces a drag error. When a moment is applied to the trunnian, the amount of lift induced deformation is changed. Also, the application of drag changes the lift induced deformation. For these reasons the error curves shown in Figure E-1 were produced. These curves give the amount of drag to be added to the raw drag output as a function of the raw drag output for various values of raw moment output.

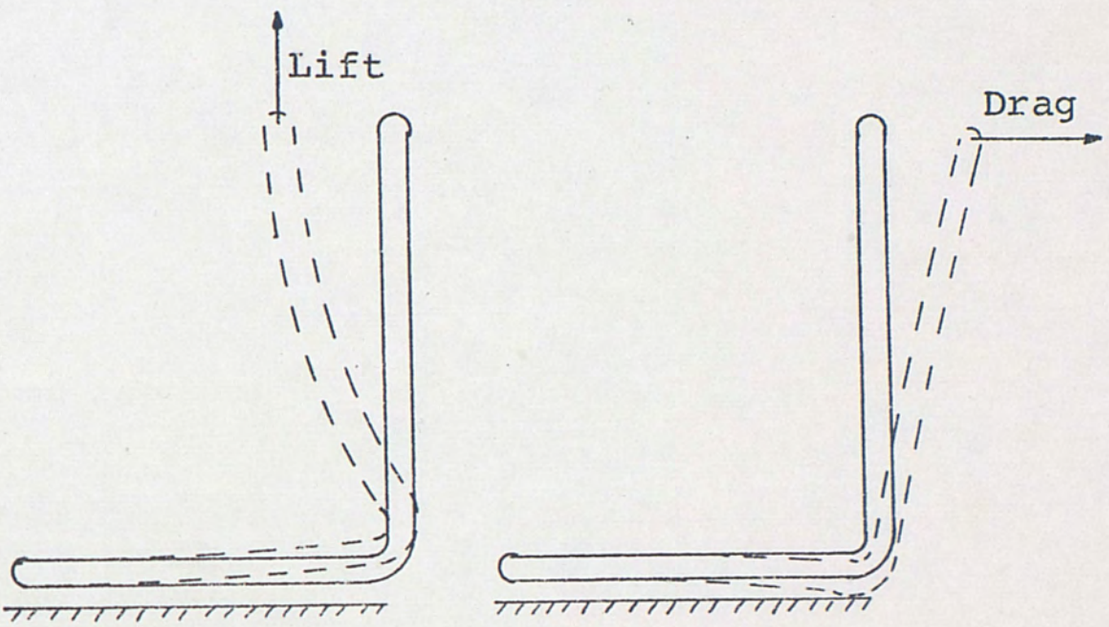


Figure 6-1, Lift and Drag Induced Beam Deformations.

# CHAPTER VII

## CONCLUSIONS

The topic of this report has been the design and analysis of a three component, single element, wind tunnel force balance. The force balance, as outlined in this report, was fabricated for use in the low speed wind tunnel at Embry-Riddle Aeronautical University at Daytona Beach, Florida. This wind tunnel is used primarily for student laboratories and the force balance has shown itself to be well suited for this use.

When the force balance was first put into operation it was noticed that the turbulence in the wind tunnel sometimes caused the model to vibrate. This was disconcerting but proved to be a small problem. It was concluded that the strain indicator null meter was only passing the lower frequencies and the meter movement is easily averaged. However, if a dynamic output becomes a testing requirement a damping system will be required.

Appendix F is the hookup instruction for the force balance at Embry-Riddle. This wind tunnel facility uses a Baldwin-Lima-Hamilton model 120C strain indicator and a Baldwin-Lima-Hamilton model 225 switching and

balancing unit. The strain gages are 3-wired to a half bridge configuration. The instructions in Appendix F apply only with this configuration using the same type equipment.

The prototype force balance has been in service for several months and its performance has been satisfactory.

# APPENDIX A

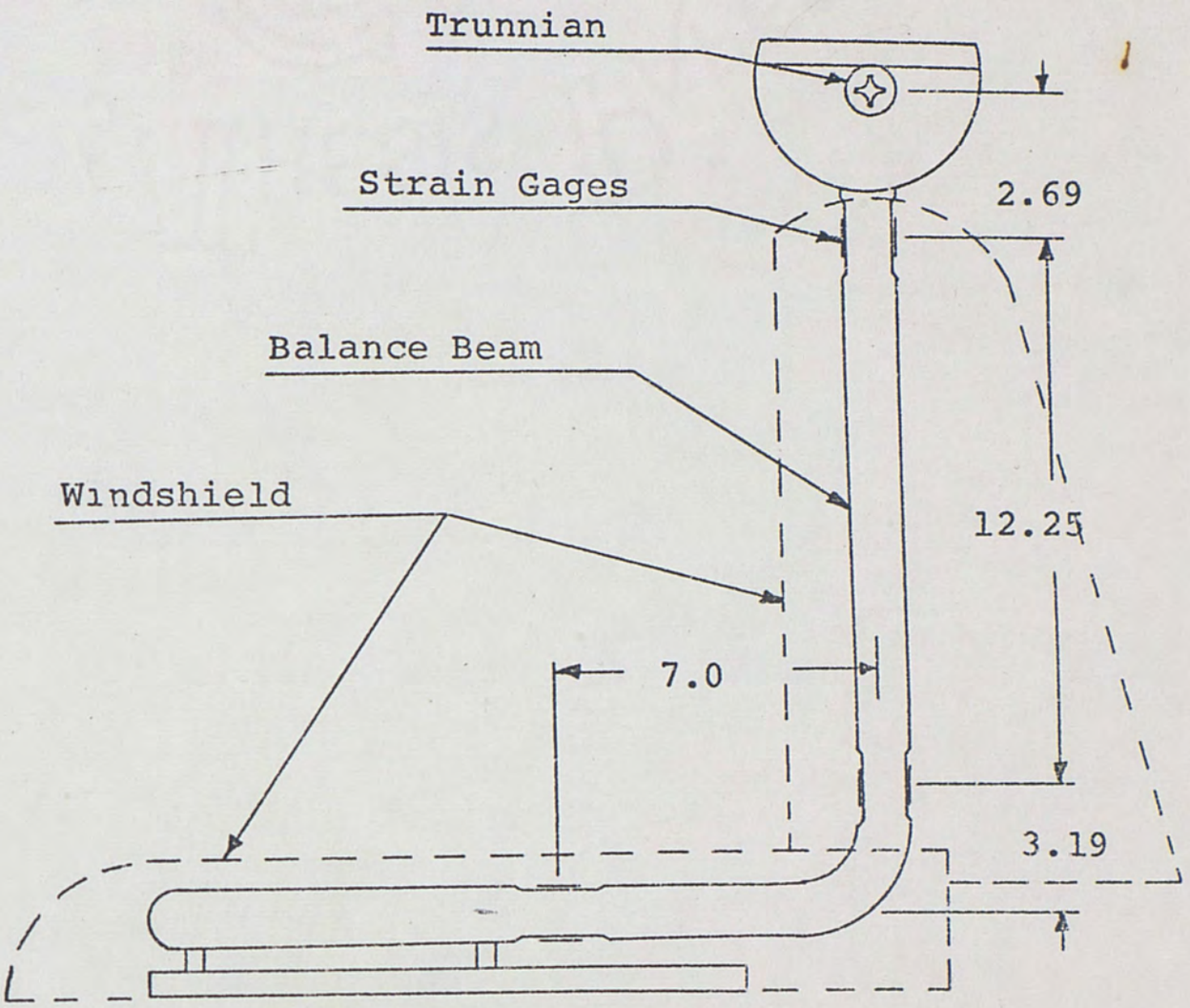


Figure A-1, Wind Tunnel Force Balance Assembly

Material: 2024 Aluminum

Strain Gages: Micro-Measurements EA-13-250BG-120

Strain Indicator: Baldwin-Lima-Hamilton, Model 120C

Switching and Balancing Unit: Baldwin-Lima-Hamilton, Model 225

# APPENDIX B

## CALIBRATION DATA

The data in the table below were taken during the calibration of the force balance. The lift and drag loads are in kilograms and the moments are one kilogram multiplied by a moment arm (inches). The data were then converted and used to draw the curves of Appendix C and Appendix E.

| Lift | Drag | Moment Arm | $R_1$ | $R_2$ | $R_3$ |
|---|---|---|---|---|---|
| 0 | 0 | 8.5 | 997 | 1000 | 1000 |
| 0 | 0 | 4.5 | 1047 | 1047 | 1047 |
| 0 | 0 | 0 | 1100 | 1100 | 1100 |
| 0 | 0 | -4.5 | 1150 | 1150 | 1151 |
| 0 | 0 | -8.5 | 1196 | 1196 | 1199 |
| 3 | 0 | -8.5 | 1193 | 1193 | 1424 |
| 3 | 0 | -4.5 | 1146 | 1146 | 1380 |
| 3 | 0 | 0 | 1097 | 1097 | 1330 |
| 3 | 0 | 4.5 | 1045 | 1046 | 1280 |
| 3 | 0 | 8.5 | 996 | 999 | 1233 |
| 6 | 0 | 8.5 | 995 | 995 | 1468 |
| 6 | 0 | 4.5 | 1040 | 1040 | 1512 |
| 6 | 0 | 0 | 1092 | 1090 | 1562 |
| 6 | 0 | -4.5 | 1143 | 1140 | 1612 |
| 6 | 0 | -8.5 | 1188 | 1184 | 1655 |

| Lift | Drag | Moment Arm | $R_1$ | $R_2$ | $R_3$ |
|---|---|---|---|---|---|
| 9 | 0 | -8.5 | 1185 | 1172 | 1886 |
| 9 | 0 | -4.5 | 1138 | 1129 | 1844 |
| 9 | 0 | 0 | 1089 | 1082 | 1795 |
| 9 | 0 | 4.5 | 1035 | 1030 | 1745 |
| 9 | 0 | 8.5 | 989 | 987 | 1702 |
| 9 | 1 | 8.5 | 951 | 803 | 1470 |
| 9 | 1 | 4.5 | 996 | 844 | 1512 |
| 9 | 1 | 0 | 1048 | 890 | 1559 |
| 9 | 1 | -4.5 | 1100 | 936 | 1606 |
| 9 | 1 | -8.5 | 1144 | 978 | 1645 |
| 9 | 2 | -8.5 | 1113 | 822 | 1452 |
| 9 | 2 | -4.5 | 1069 | 781 | 1413 |
| 9 | 2 | 0 | 1019 | 736 | 1367 |
| 9 | 2 | 4.5 | 967 | 688 | 1321 |
| 9 | 2 | 8.5 | 920 | 645 | 1281 |
| 9 | 3 | 8.5 | 892 | 497 | 1092 |
| 9 | 3 | 4.5 | 936 | 536 | 1131 |
| 9 | 3 | 0 | 988 | 583 | 1178 |
| 9 | 3 | -4.5 | 1039 | 627 | 1220 |
| 9 | 3 | -8.5 | 1085 | 667 | 1258 |
| 6 | 3 | -8.5 | 1089 | 675 | 1033 |
| 6 | 3 | -4.5 | 1044 | 635 | 991 |
| 6 | 3 | 0 | 993 | 590 | 946 |
| 6 | 3 | 4.5 | 942 | 542 | 900 |
| 6 | 3 | 8.5 | 895 | 500 | 858 |

| Lift | Drag | Moment Arm | $R_1$ | $R_2$ | $R_3$ |
|---|---|---|---|---|---|
| 6 | 2 | 8.5 | 926 | 651 | 1040 |
| 6 | 2 | 4.5 | 971 | 693 | 1089 |
| 6 | 2 | 0 | 1025 | 741 | 1135 |
| 6 | 2 | -4.5 | 1076 | 787 | 1180 |
| 6 | 2 | -8.5 | 1119 | 827 | 1220 |
| 6 | 1 | -8.5 | 1152 | 989 | 1420 |
| 6 | 1 | -4.5 | 1107 | 949 | 1381 |
| 6 | 1 | 0 | 1057 | 904 | 1335 |
| 6 | 1 | 4.5 | 1006 | 855 | 1287 |
| 6 | 1 | 8.5 | 961 | 812 | 1245 |
| 3 | 1 | 8.5 | 964 | 816 | 1010 |
| 3 | 1 | 4.5 | 1009 | 860 | 1054 |
| 3 | 1 | 0 | 1063 | 909 | 1103 |
| 3 | 1 | -4.5 | 1114 | 956 | 1149 |
| 3 | 1 | -8.5 | 1160 | 1000 | 1193 |
| 3 | 2 | -8.5 | 1126 | 837 | 991 |
| 3 | 2 | -4.5 | 1081 | 796 | 949 |
| 3 | 2 | 0 | 1030 | 751 | 903 |
| 3 | 2 | 4.5 | 979 | 702 | 854 |
| 3 | 2 | 8.5 | 933 | 659 | 812 |
| 3 | 3 | 8.5 | 900 | 499 | 613 |
| 3 | 3 | 4.5 | 946 | 541 | 654 |
| 3 | 3 | 0 | 998 | 589 | 701 |
| 3 | 3 | -4.5 | 1051 | 634 | 749 |

| Lift | Drag | Moment Arm | $R_1$ | $R_2$ | $R_3$ |
|---|---|---|---|---|---|
| 3 | 3 | -8.5 | 1094 | 676 | 790 |
| 0 | 3 | -8.5 | 1096 | 679 | 559 |
| 0 | 3 | -4.5 | 1052 | 636 | 516 |
| 0 | 3 | 0 | 1000 | 587 | 468 |
| 0 | 3 | 4.5 | 949 | 540 | 420 |
| 0 | 3 | 8.5 | 901 | 495 | 376 |
| 0 | 2 | 8.5 | 934 | 653 | 571 |
| 0 | 2 | 4.5 | 981 | 695 | 615 |
| 0 | 2 | 0 | 1031 | 745 | 662 |
| 0 | 2 | -4.5 | 1084 | 794 | 710 |
| 0 | 2 | -8.5 | 1130 | 836 | 754 |
| 0 | 1 | -8.5 | 1164 | 1001 | 961 |
| 0 | 1 | -4.5 | 1118 | 959 | 918 |
| 0 | 1 | 0 | 1065 | 911 | 869 |
| 0 | 1 | 4.5 | 1015 | 861 | 819 |
| 0 | 1 | 8.5 | 968 | 818 | 776 |

# APPENDIX C

## CALIBRATION CURVES

DVSG

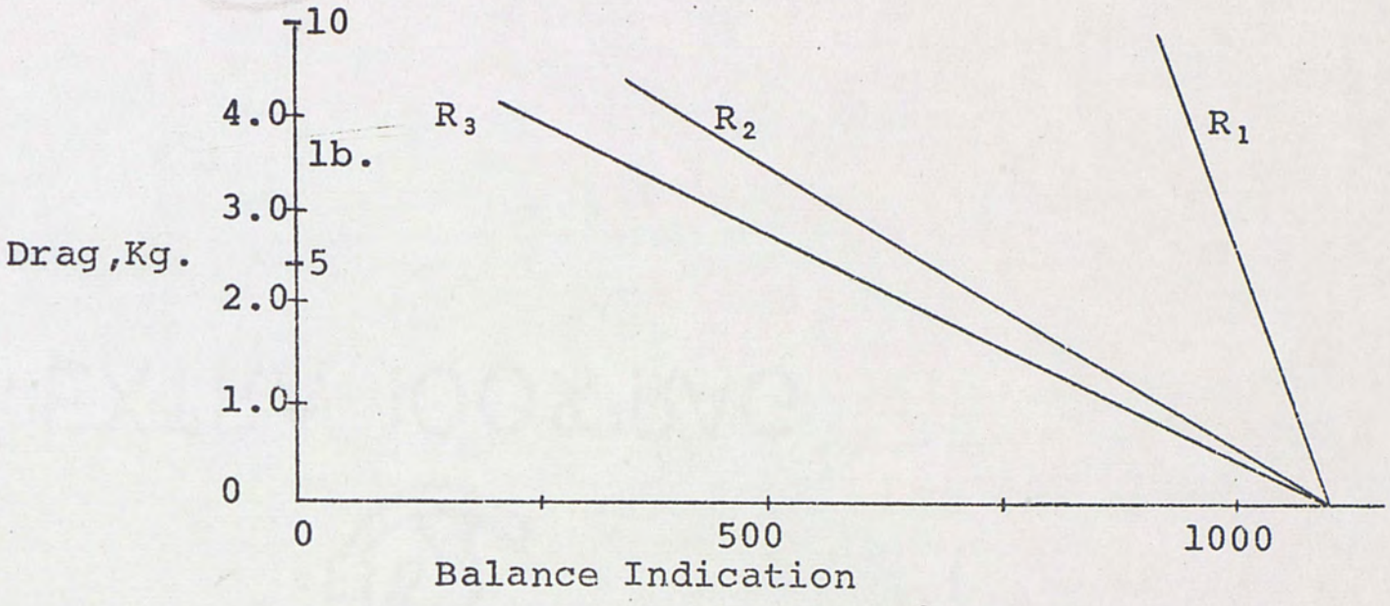


Figure C-1, Balance Indication vs Applied Drag.

LVSG

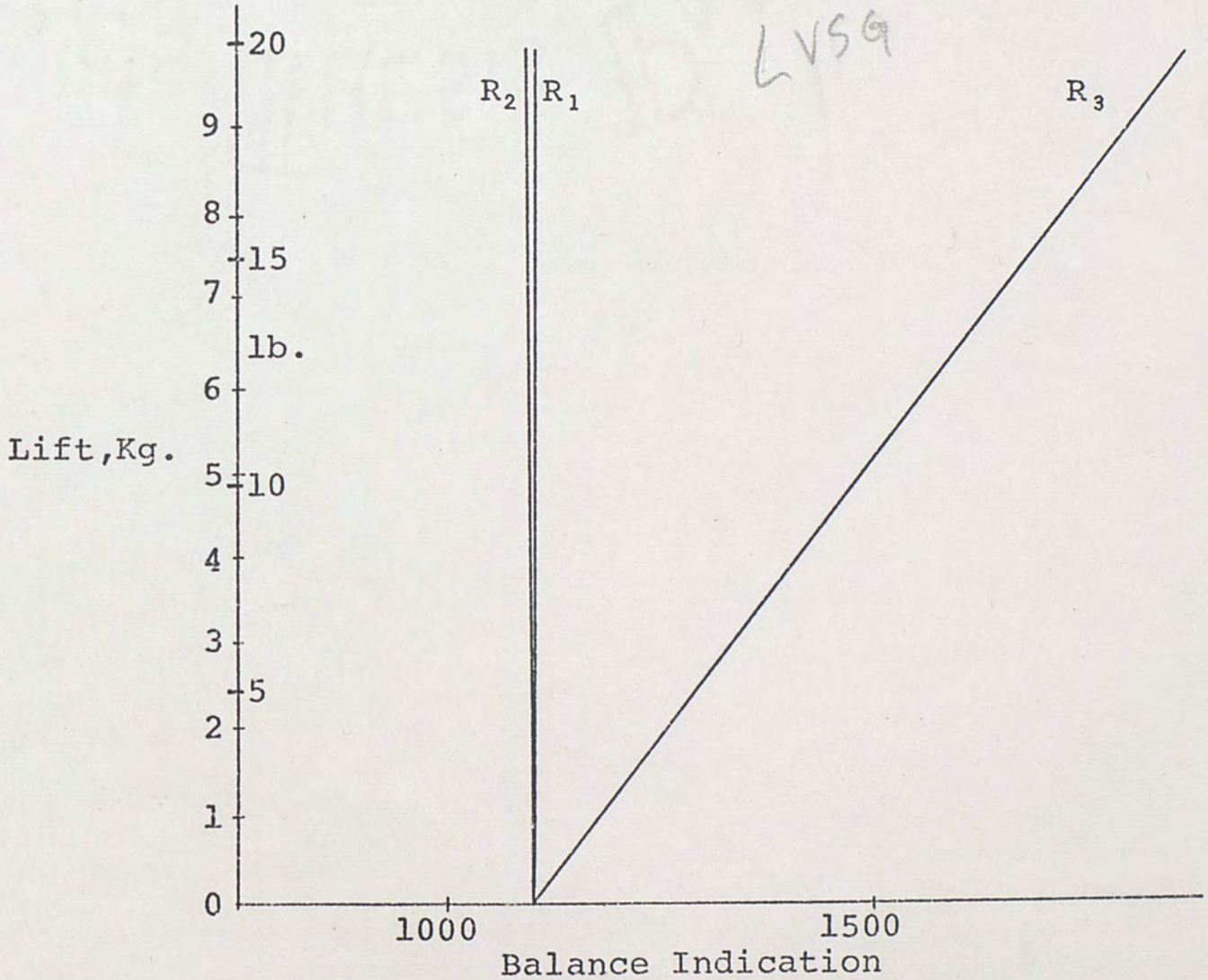


Figure C-2, Balance Indication vs Applied Lift.

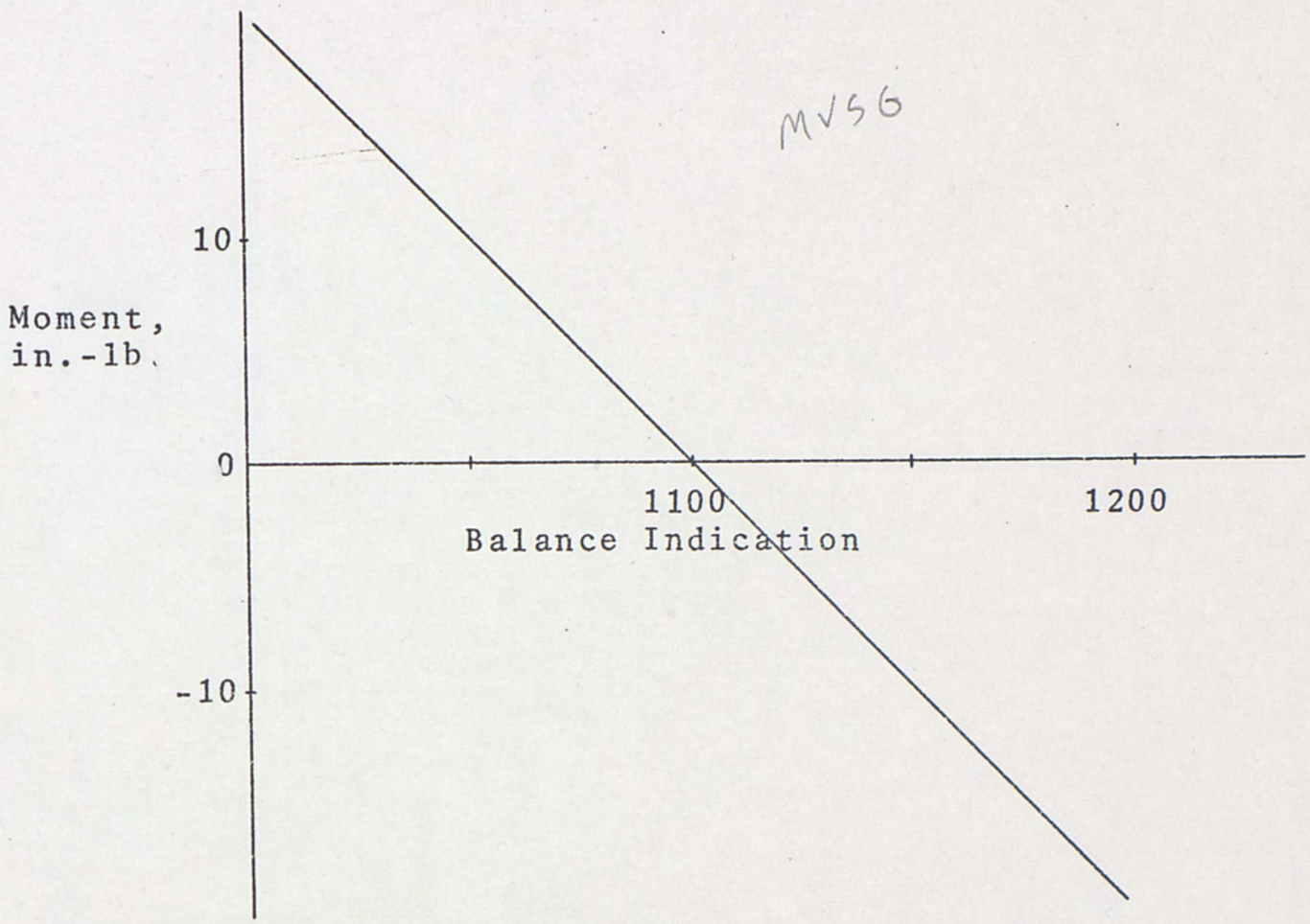


Figure C-3, Balance Indication vs Applied Moment.

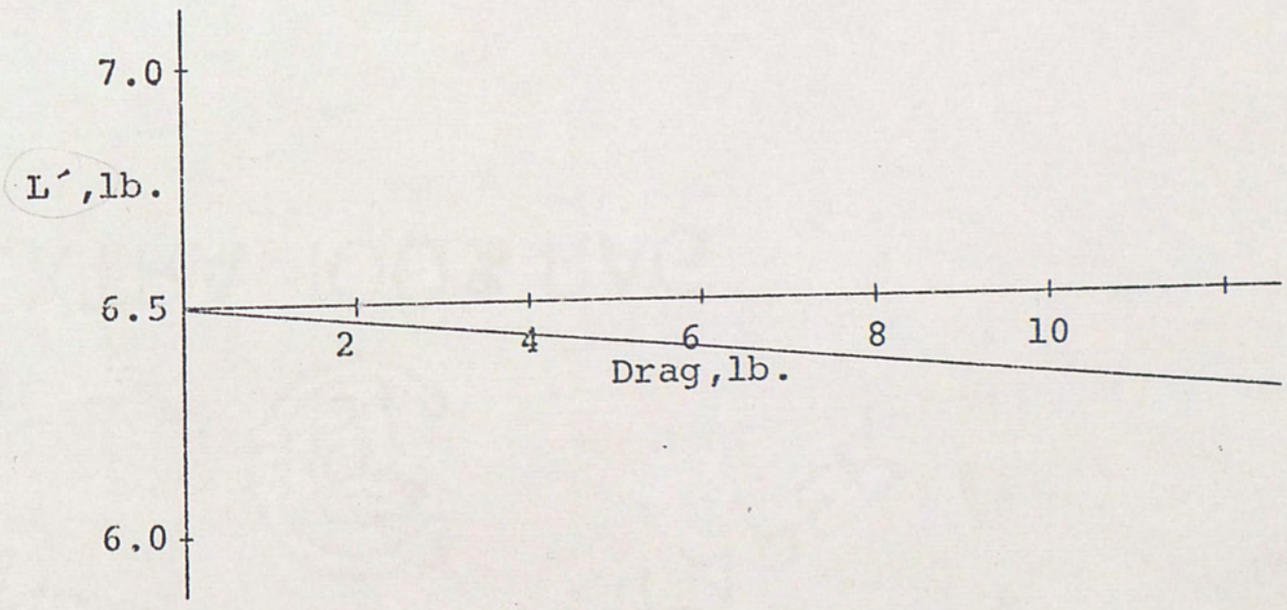


Figure C-4, Applied Drag vs Indicated Lift.

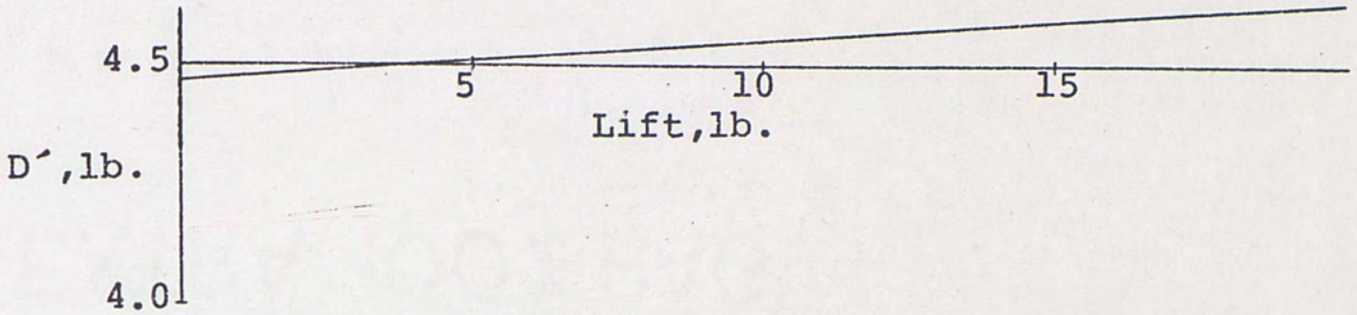


Figure C-5, Applied Lift vs Indicated Drag.

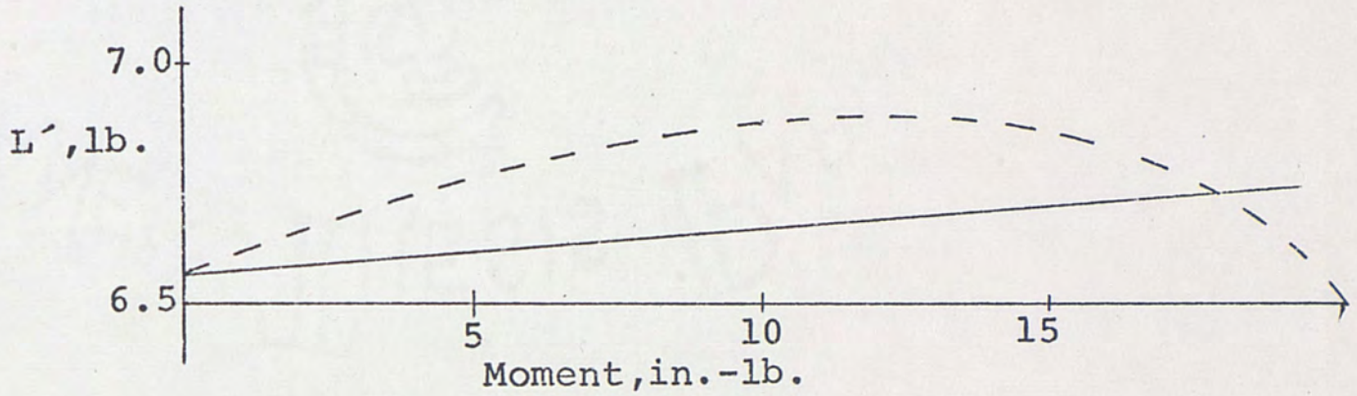


Figure C-6, Applied Moment vs Indicated Lift.

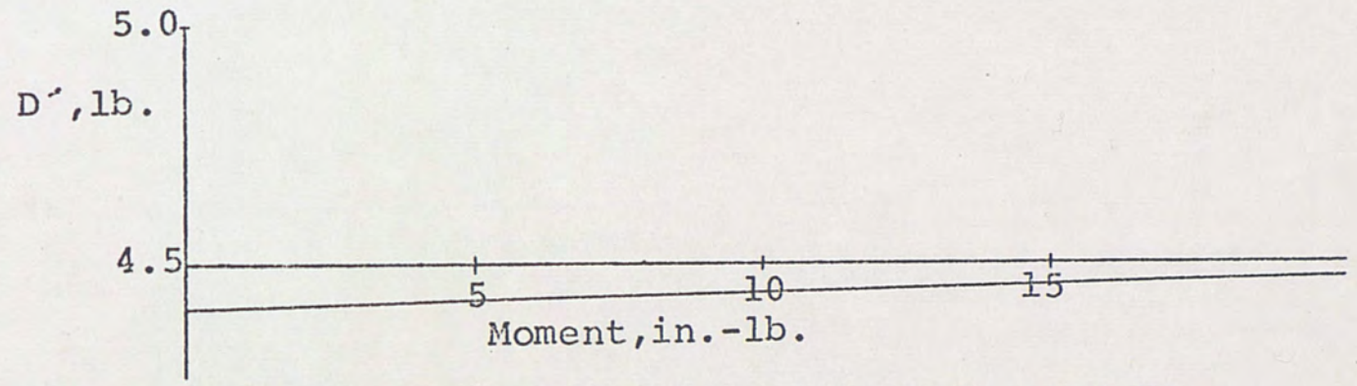


Figure C-7, Applied Moment vs Indicated Drag.

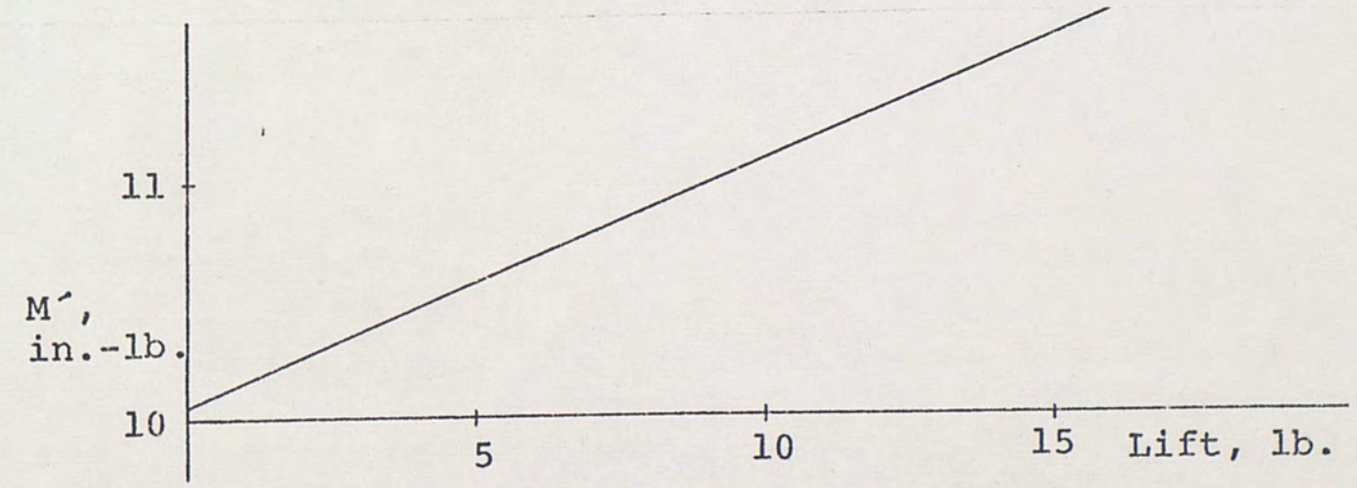


Figure C-8, Applied Lift vs Indicated Moment.

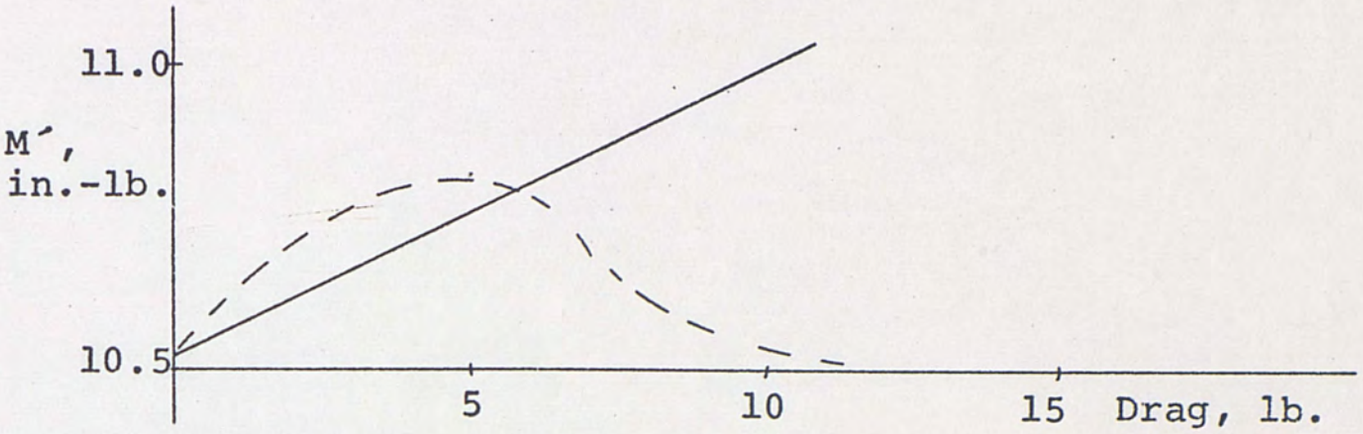


Figure C-9, Applied Drag vs Indicated Moment.

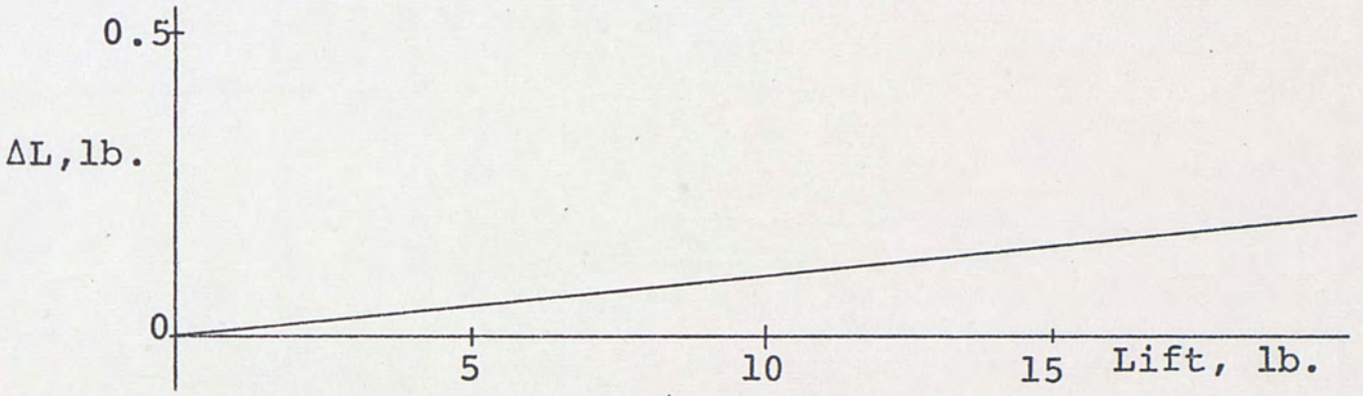


Figure C-10, Applied Lift vs Lift Error.

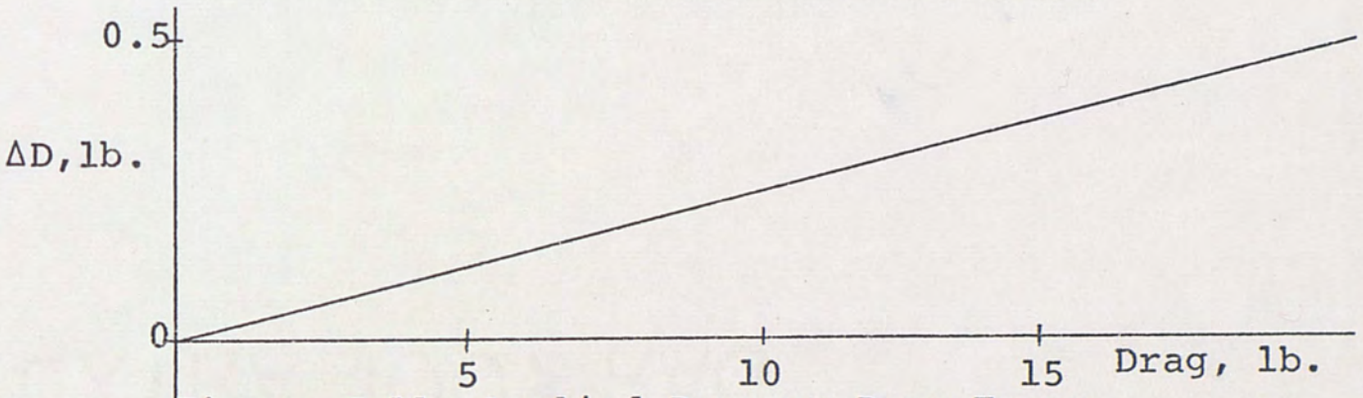


Figure C-11, Applied Drag vs Drag Error.

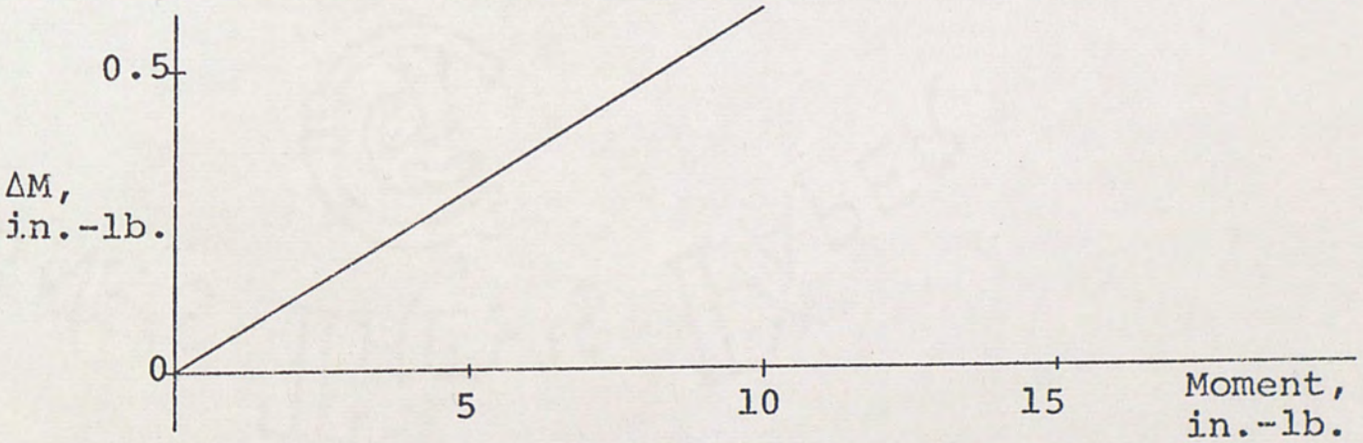


Figure C-12, Applied Moment vs Moment Error.

## APPENDIX D

## FORCE BALANCE COMPUTER PROGRAM

```
10    PRINT "WIND TUNNEL FORCE BALANCE PROGRAM"
20    PRINT "ENTER R1, R2, R3, K1, K2, K3"
30    PRINT "ENTER ZERO'S IF DATA FINISHED"
40    INPUT R1, R2, R3, K1, K2, K3
50    IF R1=0 THEN 140
60    LET L1=-.008*(K1-R1)=.0362*(K2-R2)-.0282*(K3-R3)
70    LET D1=.0162*((K2-R2)-(K1-R1))
80    LET M1=.2455*(K1-R1)-.0509*(K2-R2)
90    LET L=.9916*L1=.0191*D1-.0066*M1
100   LET D=-.0063*L1+.9523*D1-.0027*M1
110   LET M=-.0933*L1-.0314*D1+.9441*M1
120   PRINT "L=";L,"D=";D,"M=";M
130   GOTO 40
140   END
```

Note: R1, R2 and R3 are strain indicator readings.

K1, K2 and K3 are strain indicator zeros.

## APPENDIX E

## RAW DATA CORRECTION CURVES

$$L' = -.008\Delta R_1 + .0362\Delta R_2 - .0282\Delta R_3$$

$$D' = .0162(\Delta R_2 - \Delta R_1) \qquad M' = .2455\Delta R_1 - .0509\Delta R_2$$

$$L = L' \qquad D = D' + \Delta D \qquad M = M' + \Delta M$$

Note: $\Delta R_i = R_{o_i} - R_i$

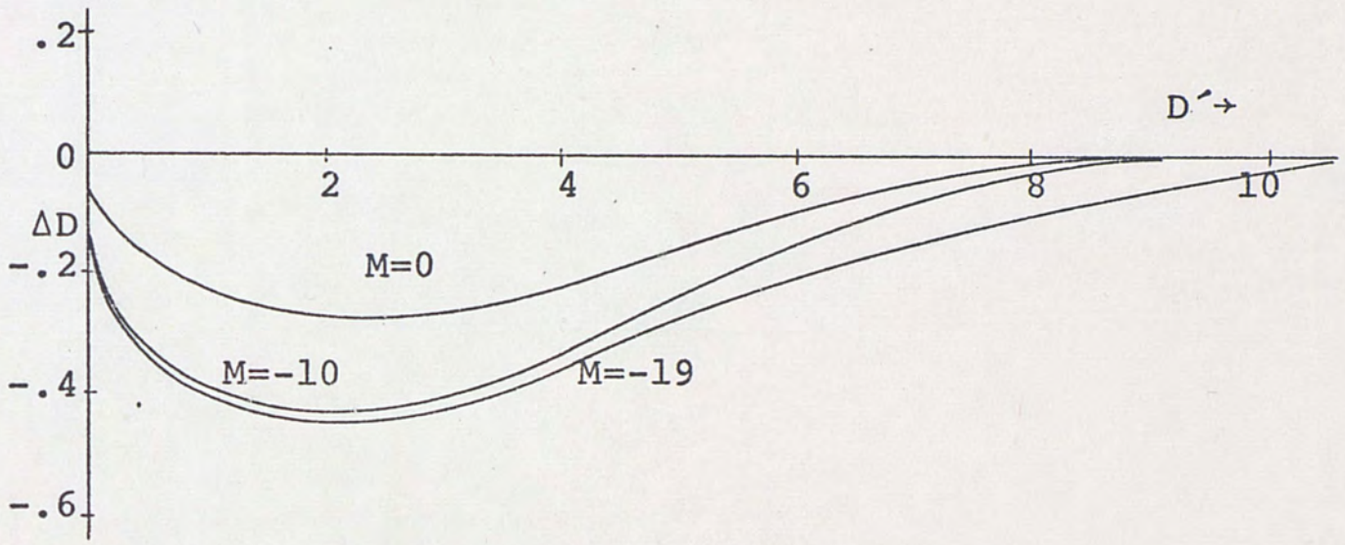


Figure E-1, Drag Compensation Curve.

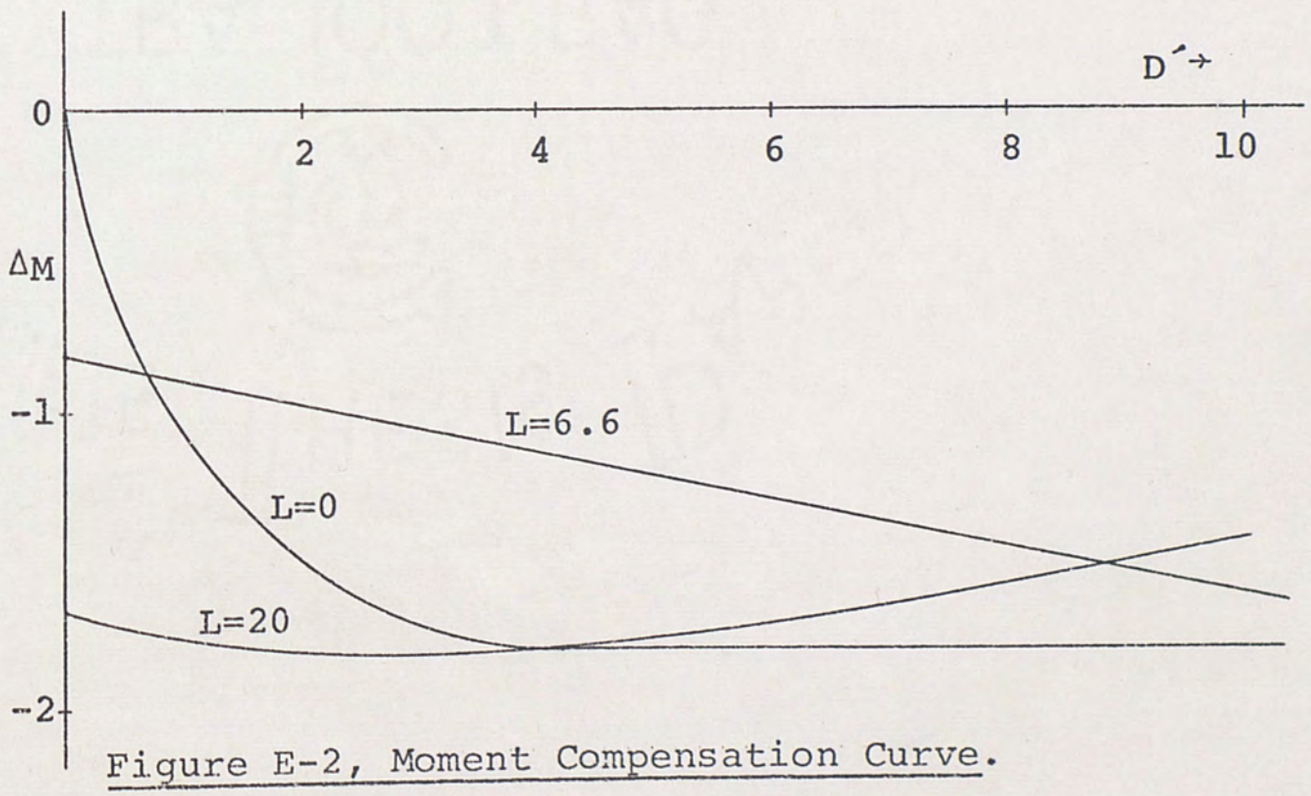


Figure E-2, Moment Compensation Curve.

## APPENDIX F

## WIND TUNNEL FORCE BALANCE HOOK-UP DIRECTIONS

BLH - Model 120C

Add to Reading 25

Micro-inches 1100

Gage Factor 2.09

Bridge Selector 4-arm

BLH - Model 225

Gage Resistance 500

Bridge Selector 2-arm

Zero Adjust #8, #9 to #10 3 turns CW

Use Channels 8, 9 and 10

Model 120C Wiring to Model 225

"4-arm" to "output" color to color

"2-arm" red to "R´"

Force Balance Wiring to Model 225

M1 to #8, M2 to #9 and M3 to #10

Black wire to "B" terminal
White wire to "W" terminal
Red wire to "G" terminal
} #8, #9 and #10

After power on, adjust the Zero Adjust knobs for channels 8, 9, & 10 to zero the null meter. Zero reading, for all three channels, is 1100 and moments will show as

a difference in readings, i.e.:

$$\Delta R = 1100 - 1000 = 100 \text{ or}$$

$$\Delta R = 1100 - 1200 = -100$$

## SELECTED REFERENCES


1. Faupel, J. H. Engineering Design.
   New York: John Wiley & Sons, 1964.

2. Gorlin, S.M., and I.I. Slezinger. Wind Tunnels and Their Instrumentation. Jerusalem: Israel Program for Scientific Translations, 1966.

3. Pope, Alan, and John J. Harper.
   Low-Speed Wind Tunnel Testing.
   New York: John Wiley & Sons, 1966.

4. Singer, F. L. Strength of Materials, 2d ed.
   New York: Harper & Row, 1962.

5. Volluz, R. J. Handbook of Supersonic Aerodynamics, Section 20, Wind Tunnel Instrumentation and Operation. NAVORD REPORT 1488, January 1961.